Quaternary Research (2017), **88**, 121–128.

doi:10.1017/qua.2017.22

Evolution of the Asian summer monsoon during Dansgaard/Oeschger events 13–17 recorded in a stalagmite constrained by high-precision chronology from southwest China

Ting-Yong Li[a,b,c]*, Li-Yin Han[a,b,c], Hai Cheng[d], R. Lawrence Edwards[e], Chuan-Chou Shen[f], Hong-Chun Li[f], Jun-Yun Li[a], Chun-Xia Huang[a], Tao-Tao Zhang[a], Xin Zhao[a]

[a]Chongqing Key Laboratory of Karst Environment, School of Geographical Sciences, Southwest University, Chongqing 400715, China
[b]State Key Laboratory of Loess and Quaternary Geology, Institute of Earth Environment, Chinese Academy of Sciences, Xi'an 710075, China
[c]Field Scientific Observation & Research Base of Karst Eco-environments at Nanchuan in Chongqing, Ministry of Land and Resources of China, Chongqing 408435, China
[d]Institute of Global Environmental Change, Xi'an Jiaotong University, Xi'an 710049, China
[e]Department of Earth Sciences, University of Minnesota, Minneapolis, Minnesota 55455, USA
[f]Department of Geosciences, National Taiwan University, Taipei 10617, Taiwan, China

(Received June 19, 2016; Accepted February 6, 2017)

Abstract

A stalagmite with high ^{238}U content from Yangkou Cave, China, revealed the evolution of the Asian summer monsoon (ASM) between 49.1 and 59.5 ka, and the $\delta^{18}O$ values recorded Dansgaard/Oeschger (D/O) events 13–17. The Yangkou record shows a relatively gradual transition into the D/O 14 and 16 events. The discrepancy between the abrupt and gradual transitions of D/O 14 in the records from northern and southern China, respectively, suggests different responses of the ASM to climate changes in the high northern latitudes. The higher resolution $\delta^{18}O$ record and more precise ^{230}Th dating indicate that the timing of D/O 14 and 17 in the Hulu records at 53 and 58 ka should be shifted to 54.3 and 59 ka, respectively. The gradual strengthening of the ASM at the onsets of D/O 16 and 14 in our record is different from the abrupt temperature rise in the northern high latitudes. Some other factors must contribute to this relatively gradual ASM change in southern China, but the actual reason is still unknown.

Keywords: Asian summer monsoon; Stalagmite $\delta^{18}O$; ^{230}Th dating; Dansgaard/Oeschger events

INTRODUCTION

One of the most important discoveries in the study of paleoclimate changes was the recognition in the early 1990s that the climate during the last glacial period was not always cold and that a series of millennial-scale climate warming events occurred, which are called Dansgaard-Oeschger (D/O) events (Johnsen et al., 1992; Bond et al., 1993; Dansgaard et al., 1993). The D/O events were abrupt changes from stadials to interstadials with durations of hundreds to thousands of years (Thomas et al., 2009). Leuschner and Sirocko (2000) and Voelker et al. (2002) summarized the geographic distribution of the D/O events on a global scale as recorded in different geologic records and indicated that the D/O events occurred worldwide.

The global footprint of the D/O events suggests that the earth system is integrated and that several interrelations and interactions occur between the ocean-atmosphere-continent systems, the Northern and Southern Hemispheres, and high and low latitudes (Bond et al., 1993; Blunier and Brook, 2001; Stocker and Johnsen, 2003; Cheng et al., 2013b). However, there are differences between the D/O events recorded in geologic archives in different latitude regions. These differences might be attributed to regional characteristics of physical environment, uncertainties in the age models, and/or resolution of records (Zhao et al., 2010). D/O events have been used as important tie points in research on the linkages between climate changes in different regions.

In this study, we reconstructed the evolution of the Asian summer monsoon (ASM) between 49.1 and 59.5 ka using a stalagmite record (JYFK7) from Yangkou Cave in Chongqing, southwest China. The improved resolution of the $\delta^{18}O$ series and the high-precision chronology of this record provide a good opportunity to study in the detail variability of

*Corresponding author at: School of Geographical Sciences, Southwest University, No. 2 Tiansheng Road, Beibei District, Chongqing 400715, China. E-mail: cdlty@swu.edu.cn (T.-Y. Li).

the ASM during this time period. By comparing the JFYK7 record with other records from northern China (Duan et al., 2016) and polar regions in the Northern Hemisphere, we investigated the response of the ASM to D/O events 13–17 during this period and assessed the different response of the ASM in northern and southern China.

GEOGRAPHIC SETTING

Stalagmite JFYK7 was collected in Yangkou Cave (29°1.68′N, 107°11.25′E; elevation: 2140 m; length: 2245 m), which is located on Jinfo Mountain (Fig. 1), Chongqing City, southwest China (Li et al., 2014). Yangkou Cave is located near the top of Jinfo Mountain, developed in Permian limestone stratum with overlying bedrock as thick as 50–100 m (Zhang et al., 1998). It is a gallery-type cave, and its width and height are generally 15–20 m (with the maximum being 64 m) and 8–12 m (with the maximum being 27 m), respectively (Zhang et al., 1998). Stalagmite JFYK7 was sampled in the south branch gallery of the cave, about 800 m and 400 m away from the entrance and the south exit, respectively (Fig. 1c).

The region has a subtropical and humid monsoon climate, which is mild and rainy. The average annual temperature is 14.5°C, and the average annual precipitation is 1435 mm. From April to October, the monthly rainfall is greater than 100 mm, and the total rainfall in this period accounts for more than 80% of the annual rainfall (Li et al., 2014; Han et al., 2016).

The top of Jinfo Mountain is surrounded by cliffs, without any surface river. All the rain and snowmelt is discharged through the karst fissures and sinkholes. Accordingly, the drip waters in Yangkou Cave are fed by local precipitation. A multiyear monitoring project was carried out in Yangkou Cave. Compared with the $\delta^{18}O$ of local precipitation ranging from −1.44‰ to −16.10‰, the $\delta^{18}O$ of drip waters (sampled

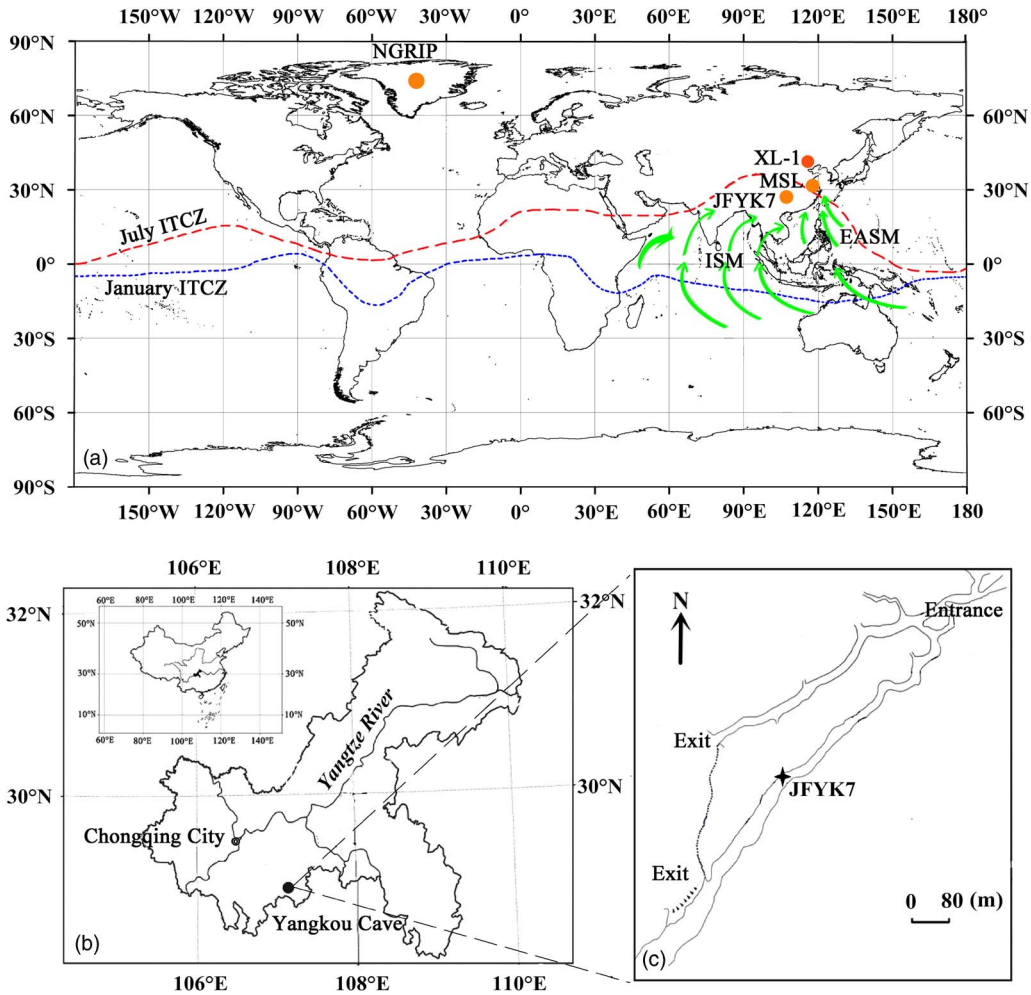

Figure 1. (a) Locations of Yangkou Cave and other sites mentioned in this study (circles) (Modified from Cheng et al., 2012). Stalagmite JFYK7 (Yangkou Cave: 29°1.68′N, 107°11.25′E) (Li et al., 2014), stalagmite XL-1 (Xinglong Cave: 40°29.21′N, 117°29.27′E) (Duan et al., 2016), stalagmite MSL (Hulu Cave: 32°3.43′N, 119°2.44′E) (Wang et al., 2001), and North Greenland Ice Core Project (NGRIP) ice core (Greenland: 75°1.00′N, 42°32.00′W) (North Greenland Ice Core project members, 2004). The current seasonal migrations of the Intertropical Convergence Zone (ITCZ; dashed lines) are denoted in red (July) and blue (January) (Lutgens and Tarbuck, 2001). The prevailing surface winds are shown by green arrows, which indicate the directions of the Indian summer monsoon (ISM) and East Asian summer monsoon (EASM) (Li et al., 2014). (b) Detail of the location of Yangkou Cave in Chongqing, China. (c) Sketch map of Yangkou Cave (after Zhang et al., 1998). (For interpretation of the references to color in this figure legend, the reader is referred to the web version of this article.)

https://doi.org/10.1017/qua.2017.22 Published online by Cambridge University Press

from six sites) in Yangkou Cave falls in the range from −7.05‰ to −9.96‰, obviously compressed by the mixing effect of overlying host rocks. The monitoring results show that no obvious evaporation occurred when precipitation infiltrated into the cave to form drips, even though drip waters in different monitoring sites lag behind local precipitation to different extents considering the difference in geologic characteristics, such as the thickness of overlying stratum and the development and connection of fissures. The $\delta^{18}O$ values of the drip water reflected the isotopic composition of the local precipitation (Wang et al., 2014). Unfortunately, no active stalagmite was collected in Yangkou Cave, nor any carbonate deposited on the glass plates placed under the drip waters in past monitoring years. Instead, some scraped powders from the surface of rocks under the drip waters can be taken as the active deposits, and the average $\delta^{18}O$ value of these deposits is −6.98‰ (Vienna Pee Dee belemnite [V-PDB]), close to the calculated value (−6.70‰) of deposits deposited at isotopic equilibrium fractionation, with the average $\delta^{18}O$ of drip waters being −8.80‰ (Vienna standard mean ocean water) and average cave temperature being 7.9°C (Li, T.-Y., unpublished data). In spite of this, the $\delta^{18}O$ values of the local precipitation showed clear seasonal variations that were strongly influenced by the summer monsoon, with light values in summer and heavier values in winter (Wang et al., 2014). Consequently, the $\delta^{18}O$ values of the stalagmite can be used to assess the variability of the summer monsoon; low stalagmite $\delta^{18}O$ values denote a stronger summer monsoon and vice versa (Cheng et al., 2009; Liu et al., 2013; Li et al., 2014; Zhou et al., 2014; Han et al., 2016).

ANALYTIC METHODS

Stalagmite JFYK7 has a cylindrical shape and is approximately 125 mm and 40 mm in diameter at the bottom and top, respectively. The stalagmite was cut in half along the growth axis. The vertical section is dark brown, and growth banding is clearly visible. Measured along the growth axis, stalagmite JFYK7 is 555 mm long, and the section between 193 mm and 399 mm is discussed in this study. Fifteen subsamples were drilled for ^{230}Th dating from the polished surface of JFYK7 using carbide dental burrs with a diameter of 1 mm. The subsamples were ^{230}Th dated by multicollector inductively coupled plasma mass spectrometry in the Isotope Laboratories of the University of Minnesota and Xi'an Jiaotong University. The age errors are given in two standard deviations (2σ) (Edwards, 1988; Shen et al., 2012; Cheng et al., 2013a). The decay constants of ^{230}Th, ^{234}U, and ^{238}U are 9.1705×10^{-6}/yr (Cheng et al., 2013a), 2.82206×10^{-6}/yr (Cheng et al., 2013a), and 1.55125×10^{-6}/yr (Jaffey et al., 1971), respectively. The age correction for the initial ^{230}Th was performed using the average crustal $^{230}Th/^{232}Th$ ratio of $4.4 \pm 2.2 \times 10^{-6}$ (Taylor and McLennan, 1995).

The $\delta^{18}O$ and $\delta^{13}C$ analyses of JFYK7 were performed in the Geochemistry and Isotope Laboratory of Southwest University, China. A total of 413 subsamples were drilled for isotope analysis along the growth axis using a 0.5-mm-diameter drill bit and a sampling interval of 0.5 mm. The analyses were performed using a Delta V Plus mass spectrometer, which was combined with a Kiel IV Carbonate Device. Every seven samples were bracketed with one work standard (SWU1). The isotopic results are given with respect to the V-PDB standard with a 1-sigma external error $<\pm 0.1$‰ for $\delta^{18}O$ and $<\pm 0.06$‰ for $\delta^{13}C$ (Li et al., 2011).

The spectral analysis was performed on the $\delta^{18}O$ records of JFYK7 using the program REDFIT 37. This software allows the variance of a time series to be separated into contributions associated with different time scales, which is useful for better understanding the origins of the variability recorded in a time series (Schulz and Mudelsee, 2002).

RESULTS

^{230}Th dating

The dating results are shown in Table 1. Because the concentration of ^{238}U in the stalagmites from Yangkou Cave is approximately 10 ppm (Li et al., 2014; Han et al., 2016), the dating precision for JFYK7 is high, and all of the age errors are less than ±200 yr. The $^{230}Th/^{232}Th$ ratio is another important factor that affects the dating precision (Shen et al., 2012). The ^{230}Th /^{232}Th ratio is as high as 27,000 to 970,000 x 10^{-6} (Table 1). Thus, it is not necessary to correct the results using the initial ^{230}Th, and the age errors are less than 0.4%. In this study, all ages are in the stratigraphic order, and a linear interpolation method was used to establish an age-depth model (Fig. 2). The timing for the section of JFYK7 discussed in this study (193 to 399 mm in depth) is in the period of 49–59 ka, and the average resolution for the $\delta^{18}O$ record is 24 yr.

Carbon and oxygen isotopes

Previous work on stalagmite JFYK7 indicated that it was deposited under isotope equilibrium fractionation conditions and that the variation of $\delta^{18}O$ was mainly controlled by climatic factors (Han et al., 2016). Although both the $\delta^{18}O$ and $\delta^{13}C$ values shows large changes at century to millennial time scales, the details show several significant differences (Fig. 3). During the period from 49.1 to 59.5 ka, the $\delta^{18}O$ values of JFYK7 fluctuate between −9.8‰ and −7.0‰ with an average of −8.4‰. The maximum and minimum $\delta^{18}O$ values occurred at approximately 55.0 and 52.3 ka, respectively (Fig. 3).

Spectral analysis

Spectra of paleoclimatic time series frequently show a continuous decrease of spectral amplitude with increasing frequency ("red noise") (Schulz and Mudelsee, 2002). The red noise test showed that periods of 144 yr and 125 yr are statistically significant periodicities in the $\delta^{18}O$ data at the

https://doi.org/10.1017/qua.2017.22 Published online by Cambridge University Press

Table 1. Inductively coupled plasma mass spectrometry dating results of stalagmite JFYK7.

Sample number	Depth (mm)	^{238}U (ppb)	^{232}Th (ppt)	$\delta^{234}U_{initial}$ (corrected)	$^{230}Th/^{238}U$ (activity)	$^{230}Th/^{232}Th$ (10^{-6})	^{230}Th age (ka, corrected)
JFYK7-10	209.5	12,395 ± 19.5	239 ± 14	51.8 ± 2.2	0.3883 ± 0.0008	331,665 ± 19,015	49.961 ± 0.195
JFYK7-11	213	11,317 ± 13.3	2645 ± 62	56.9 ± 2.0	0.3929 ± 0.0007	27,721 ± 652	50.383 ± 0.176
JFYK7-1515	234	12,101 ± 12.6	166 ± 7	36.8 ± 1.2	0.3864 ± 0.0005	464,335 ± 18,938	50.622 ± 0.118
JFYK7-1516	262.5	14,787 ± 16.7	100 ± 6	45.0 ± 1.3	0.3994 ± 0.0006	969,049 ± 60,134	52.240 ± 0.127
JFYK7-12	284	12,505 ± 16.6	209 ± 19	34.2 ± 2.0	0.3983 ± 0.0007	392,092 ± 36,060	52.816 ± 0.190
JFYK7-13	287	11,324 ± 13.8	254 ± 23	31.3 ± 2.0	0.3991 ± 0.0007	293,135 ± 26,041	53.141 ± 0.190
JFYK7-1517	314	8943 ± 8.5	322 ± 9	34.8 ± 1.3	0.4079 ± 0.0006	186,812 ± 5121	54.411 ± 0.139
JFYK7-1518	324	7517 ± 7.1	637 ± 14	38.5 ± 1.3	0.4141 ± 0.0005	80,541 ± 1754	55.214 ± 0.135
JFYK7-14	331.5	12,406 ± 15.8	338 ± 21	41.5 ± 2.0	0.4185 ± 0.0007	253,126 ± 15,438	55.747 ± 0.195
JFYK7-15	334	11,546 ± 15.6	849 ± 17	29.5 ± 1.6	0.4154 ± 0.0007	93,186 ± 1886	56.124 ± 0.179
JFYK7-1519	351	10,111 ± 9.6	256 ± 8	40.0 ± 1.3	0.4266 ± 0.0006	278,180 ± 8436	57.285 ± 0.143
JFYK7-1520	367	6933 ± 6.5	328 ± 9	27.5 ± 1.3	0.4252 ± 0.0006	148,372 ± 4233	58.007 ± 0.149
JFYK7-1521	382.5	9240 ± 8.7	191 ± 7	6.3 ± 1.3	0.4214 ± 0.0006	335,513 ± 11,756	59.063 ± 0.151
JFYK7-1522	394	13,984 ± 14.2	156 ± 7	18.8 ± 1.3	0.4285 ± 0.0006	634,477 ± 28,407	59.336 ± 0.149
JFYK7-16	399.0	13,763 ± 15.8	222 ± 16	17.8 ± 1.7	0.4288 ± 0.0007	438,464 ± 31,977	59.469 ± 0.191

Notes: $^{230} = 9.1705 \times 10^{-6}$/yr; $\lambda^{234} = 2.82206 \times 10^{-6}$/yr; $\lambda^{238} = 1.55125 \times 10^{-10}$/yr.
$\delta^{234}U = ([^{234}U/^{238}U]_{activity} - 1) \times 1000$.
$\delta^{234}U_{initial}$ was calculated based on ^{230}Th age (T) (i.e., $\delta^{234}U_{initial} = \delta^{234}U_{measured} \times e^{\lambda 234 \times T}$).
Corrected ^{230}Th ages assume the initial $^{230}Th/^{232}Th$ atomic ratio of $4.4 \pm 2.2 \times 10^{-6}$. Those are the values for a material at secular equilibrium, with the bulk earth $^{232}Th/^{238}U$ value of 3.8. The errors are arbitrarily assumed to be 50%.

95%–99% confidence level (Fig. 4). The 144 yr period reflects the century-scale period in the interstadials during D/O events 13–17, which is approximately consistent with the 148 yr cycle of ^{14}C recorded by tree rings (Stuiver and Braziunas, 1993). The 125 yr period reflects the solar cycle as has been observed in other paleoclimate records (Stuiver and Braziunas, 1989; Castagnoli et al., 1990; Agnihotri et al., 2002). In addition, there are statistically significant periodicities at the 99% confidence level of 133, 81, 73, 67, 62, 57, and 53 yr (Fig. 4). Based on the resolution of the $\delta^{18}O$ record (~24 yr), most of the cycles, such as 73, 67, 62, 57, and 53 yr, may simply be because of random fluctuations. Only the 133 yr and 81 yr cycles can be trusted. The 133 yr period is known from ^{14}C data of tree-ring records (Damon and Sonnett, 1991). The 81 yr cycle is consistent with the solar centennial cycles (70–100 yr, the Gleissberg cycle) and was also identified in Chinese stalagmites (Dykoski et al., 2005).

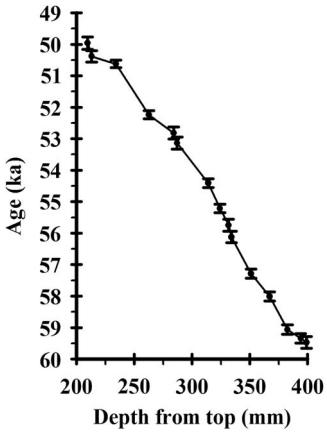

Figure 2. Age-depth model of stalagmite JFYK7 based on linear interpolation.

DISCUSSION

Difference between northern and southern Chinese stalagmite records

A recent stalagmite record from northern China, which covers the change of the ASM during D/O 14 and 15, shows abrupt onsets of D/O 14 and 15.2 and strongly resembles those of the North Greenland Ice Core Project (NGRIP) record (Fig. 5b; Fig. 2 in Duan et al., 2016). The abrupt transition into D/O 14 is significantly different from the relatively gradual change in our record and MSL,

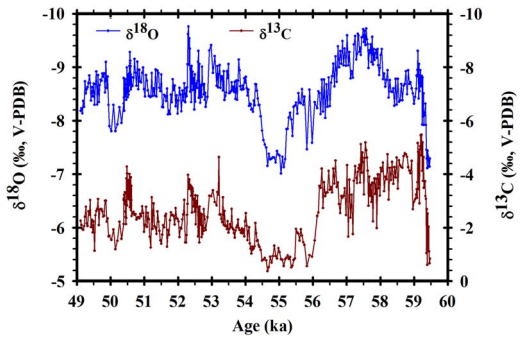

Figure 3. (color online) The $\delta^{18}O$ and $\delta^{13}C$ records of stalagmite JFYK7.

https://doi.org/10.1017/qua.2017.22 Published online by Cambridge University Press

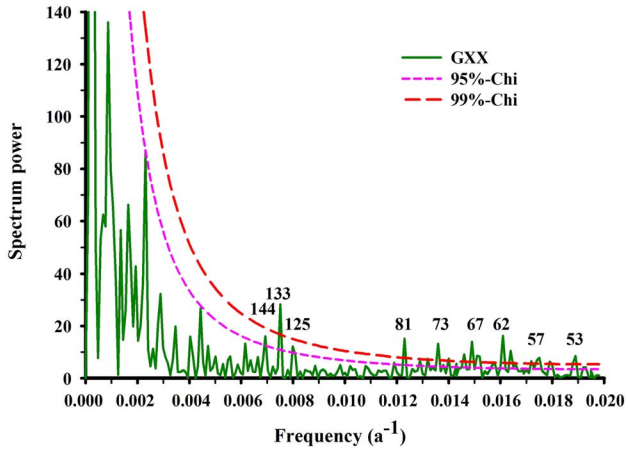

Figure 4. Spectral analysis (Schulz and Mudelsee, 2002) (green solid line) of the $\delta^{18}O$ records of stalagmite JFYK7 from Yangkou Cave. GXX is the spectrum of the data, and 95%-Chi (pink short dashed curve) and 99%-Chi (red long dashed curve) are the 95% and 99% confidence levels, respectively. (For interpretation of the references to color in this figure legend, the reader is referred to the web version of this article.)

which is from Hulu Cave in eastern China (Wang et al., 2001) (Fig. 5c and d, Fig. 6). In spite of the resolution difference in $\delta^{18}O$ and chorology, the duration for the transition of D/O 14 in the records of NGRIP (Svensson et al., 2008), XL-1 (Duan et al., 2016), JFYK7 (this study), and MSL (Wang et al., 2001) is 40, 110, 360, and 400 yr, respectively (Fig. 6). The transition of D/O 14 recorded in northern China is obviously faster than that in southern China.

We speculate that this discrepancy between northern and southern China may have been caused by the different responses to climate changes in the high northern latitudes. The westerlies have been proposed as the linkage for rapid atmospheric teleconnection between the North Atlantic and ASM regions (Porter and An, 1995), which mainly influence the middle latitudes of the Northern Hemisphere (Railsback et al., 2014). The Yangkou and Hulu Caves located in southern China and meteoric observations confirmed that during the summer months, the moisture from the Indian Ocean, the South China Sea, and the western Pacific affects southern China (Ding et al., 2004). Thus, climate change in southern China is not only influenced by the high northern latitudes, but also may be modulated by changes in the tropical oceans (Li et al., 2014; Zhao et al., 2016). In other words, the differences in climate change patterns between northern and southern China presented in stalagmites may be attributed to the differences of the influence on these two regions from climate change in the northern high latitudes, the tropical Indian Ocean, and the Pacific Ocean.

Climate events D/O 13–17 recorded in JFYK7 are similar to those in the MSL stalagmite record, especially the gradual decreases of the ASM at the end of D/O 16 and at the onset of D/O 14 (Fig. 5c and d). This similarity suggests synchronous changes of the ASM in eastern and southwestern China from 49.1 to 59.5 ka.

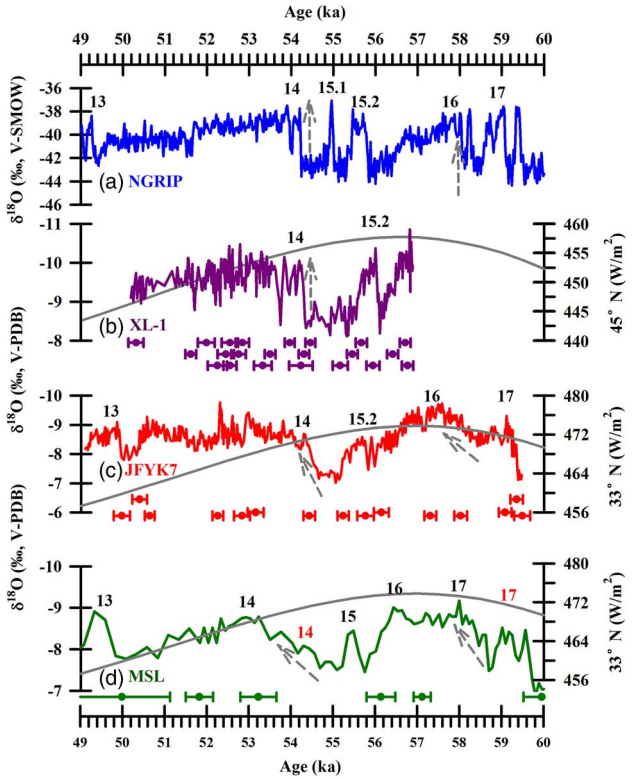

Figure 5. Comparison between the stalagmite $\delta^{18}O$ record from Yangkou Cave and other records. (a) $\delta^{18}O$ of North Greenland Ice Core Project (NGRIP; Svensson et al., 2008). (b) $\delta^{18}O$ of stalagmite XL-1 from Xinglong Cave (Duan et al., 2016). (c) $\delta^{18}O$ of stalagmite JFYK7 from Yangkou Cave in southwestern China (this study). (d) $\delta^{18}O$ of stalagmite MSL from Hulu Cave in Nanjing, China (Wang et al., 2001). We suggest that the initial signature of Dansgaard/Oeschger 14 and 17 in the MSL record should be shifted to 54.3 and ~59 ka, which is presented by the arabic numerals 14 and 17 in red, respectively. The gray curves denote the variation of summer insolation (Berger, 1978; Berger and Loutre, 1991; Paillard et al., 1996; Laskar et al., 2004). ^{230}Th dates and age uncertainties for the stalagmite records XL-1, JFYK7, and MSL are shown in the corresponding colors. The gray dashed lines with an arrow denote the trend of changes in different records. V-PDB, Vienna Pee Dee belemnite; V-SMOW, Vienna standard mean ocean water. (For interpretation of the references to color in this figure legend, the reader is referred to the web version of this article.)

Although the overall changes in the JFYK7 and MSL records are in broad agreement, there are several small-scale differences (Fig. 5c and d). First, in the JFYK7 record, the start and end of D/O 17 occurred at ~59.3 ± 0.2 and ~58.4 ± 0.2 ka BP, respectively, and the start and end of D/O 16 occurred at ~58.4 ± 0.2 and ~56.0 ± 0.2 ka, respectively; the duration of D/O 16, therefore, was approximately 2.4 ka. However, the corresponding dates in the MSL records are ~58.7 ± 0.3 and ~57.4 ± 0.2 ka, and ~57.4 ± 0.2 and ~55.8 ± 0.4 ka, respectively, indicating the duration of D/O 16 was 1.6 ka (Wang et al., 2001). Second, the $\delta^{18}O$ values of JFYK7 and MSL gradually become more negative at the onset of D/O 16, and the amplitudes of the $\delta^{18}O$ fluctuations were

https://doi.org/10.1017/qua.2017.22 Published online by Cambridge University Press

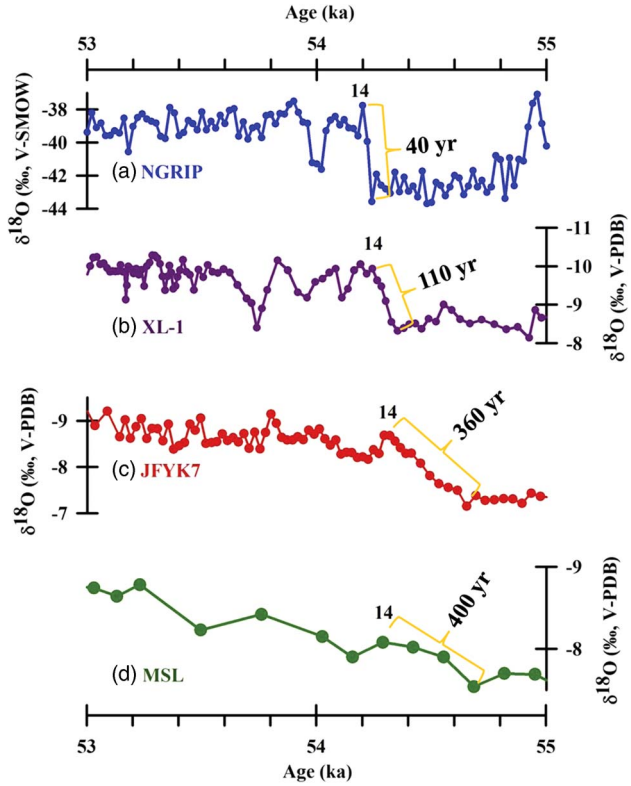

Figure 6. (color online) Expanded comparison for the transition of Dansgaard/Oeschger 14 between the stalagmite $\delta^{18}O$ record from Yangkou Cave and other records. (a) $\delta^{18}O$ of North Greenland Ice Core Project (NGRIP; Svensson et al., 2008). (b) $\delta^{18}O$ of stalagmite XL-1 from Xinglong Cave (Duan et al., 2016). (c) $\delta^{18}O$ of stalagmite JFYK7 from Yangkou Cave in southwestern China (this study). (d) $\delta^{18}O$ of stalagmite MSL from Hulu Cave in Nanjing, China (Wang et al., 2001).

approximately 1.4‰ and 0.4‰, respectively. In contrast, after the peak of D/O 16, the $\delta^{18}O$ values gradually become less negative and reach maximum values in JFYK7 and MSL within 1.5 ka and 0.6 ka, respectively. Third, during D/O 14, a notable bimodal pattern is recorded in JFYK7, but the MSL record shows a single symmetrical pattern (Fig. 5b and c). The strongest summer monsoon during the peak of D/O 14 recorded in JFYK7 occurred at ~52.3 ± 0.1 ka compared with ~53.2 ± 0.4 ka in the MSL record. The $\delta^{18}O$ values of stalagmite MSL gradually become more negative at the start of D/O 14, reach the minimum value at ~53.2 ± 0.4 ka, and then gradually become less negative (Fig. 5d). This symmetrical pattern during D/O 14 in the MSL $\delta^{18}O$ records is not fully reflected in the JFYK7 record (Fig. 5c).

Compared with the MSL record, the JFYK7 record provides more details about the evolution of the ASM during this period because of the higher $\delta^{18}O$ resolution (~24 yr) and the better chronology because of more ^{230}Th dates and higher dating precision (Fig. 5c and d). The series of D/O events in JFYK7 is more similar to the NGRIP record (Fig. 5a, c, and d). We propose that the original identification of D/O 17 in MSL at ~58 ka should be shifted to ~59 ka and that the original D/O events 16 and 17 should belong to D/O 16 (Fig. 5d). In addition, the original identification of D/O 14 in MSL at ~53 ka should be shifted to ~54.3 ka (Fig. 5d). The MSL record will then be more consistent with the JFYK7 and NGRIP records.

The consistency between JFYK7 and MSL may partly be attributed to the change of solar insolation in the Northern Hemisphere, which influenced the evolution of the ASM. On the other hand, the discrepancies in the patterns and phases of $\delta^{18}O$ records from JFYK7 and MSL should be attributed to the regional differences within the summer monsoon regimes, such as the individual characteristics of the caves, vegetation feedbacks, and others that could dampen the abrupt signals, and/or uncertainties in the age models and resolution of different records (Zhao et al., 2010).

Comparison with NGRIP

Five $\delta^{18}O$ excursions in the JFYK7 records correspond to centennial- to millennial-scale climatic oscillations (D/O events 13–17) that have been documented in the Greenland ice cores (Fig. 5). The $\delta^{18}O$ values of Greenland ice cores are mainly influenced by the local air temperature (Dansgaard, 1954; Dahl-Jensen and Johnsen, 1986; Jouzel et al., 1997; Thomas et al., 2009). This suggests coupling between the ASM and the temperature changes over the North Atlantic. In general, the ASM recorded in JFYK7 was intensified/weakened when the temperatures recorded in the NGRIP cores increased/decreased (Fig. 5a and c). The westerlies have been proposed as the linkage between the ASM and climate changes in the high latitudes of the Northern Hemisphere (Porter and An, 1995; Cosford et al., 2008). This mechanism was confirmed by a simulation that coupled the North Atlantic meridional overturning circulation and the East Asian monsoon (Sun et al., 2012).

Despite the overall similarity between JFYK7 and NGRIP, there are several differences. The temperature changes recorded in the NGRIP record show abrupt increases at the onsets of D/O 16 and 14 (Fig. 5a) (North Greenland Ice Core Project members, 2004), in contrast to the relatively gradual increase recorded by JFYK7 (Fig. 5c). In addition, the temperature changes indicate rapid cooling at the ends of D/O events 17 and 15 (Fig. 5a), but this pattern was not prominent in the variation of ASM recorded by JFYK7 (Fig. 5c). Other discrepancy between JFYK7 and NGRIP is the absence of D/O 15.1 in JFYK7 record, similar to the record from northern China (Fig. 5b) (Duan et al., 2016).

The abrupt temperature changes recorded in the NGRIP record at the onsets of D/O 16 and 14 and the onsets and ends of D/O 17 and 15 are tightly related to the climate changes around the North Atlantic, whereas the Asian monsoon system is mainly driven by the thermal contrast between the Indian Ocean, the Pacific Ocean, and the Asian continent (Webster et al., 1998; Wang and Lin, 2002). Yangkou Cave is located in the mid-low latitudes of the Asian monsoon region, which is influenced by the Indian summer monsoon and the East Asian summer monsoon (Fig. 1a) (Ding et al.,

https://doi.org/10.1017/qua.2017.22 Published online by Cambridge University Press

2004; Li et al., 2007). Previous studies indicate a rapid atmospheric teleconnection between the North Atlantic and the ASM (Porter and An, 1995; Sun et al., 2012; Duan et al., 2016); other factors must have modulated the evolution of the ASM and resulted in the discrepancies between China and Greenland. The tropical Indian Ocean, the Pacific Ocean, even temperature changes in the Southern Hemisphere have been deemed to modulate the evolution of the ASM (Cai et al., 2006; Li et al., 2014; Zhou et al., 2014, 2016; Han et al., 2016), but the credible and convincing mechanism remains unclear.

CONCLUSIONS

A new, high-precision stalagmite $\delta^{18}O$ record from southwest China, JFYK7, revealed the evolution of the ASM between 49.1 and 59.5 ka and reproduced the D/O 13–17 events that have been documented in the Greenland ice cores. The new record shows more details about the changes of the ASM and revises the previous identification of D/O 14 and 17 from 53 to 54.3 ka and 58 to 59 ka, respectively. The different pattern of the stalagmite records from northern China (Duan et al., 2016) and southern China (JFYK7)—for example, with respect to the onset of D/O 14 and 16—suggests a different response of the ASM to climate change in the high northern latitudes. Further research is needed to clarify the influence on the ASM of the climate changes in tropical oceans and the Southern Hemisphere.

ACKNOWLEDGMENTS

Great thanks to the editors Matthew Lachniet and Derek Booth and the anonymous reviewers for their constructive suggestions and comments to improve the manuscript. A professional English translator, Dr. Xiang Xinyi, Southwest University, China, is also greatly appreciated for her effort in polishing the manuscript. This research was supported by National Natural Science Foundation of China (Nos. 41172165, 41302138, and 41440020), "the Fundamental Research Funds for the Central Universities" (Nos. XDJK2013A012, XDJK2014C010, and XDJK2017A010), "Karst Dynamics Laboratory, MLR and GZAR" (No. KDL201301), and the open project of the "State Key Laboratory of Loess and Quaternary Geology" (No. SKLLQG1310) to T.-Y. Li and J.-Y. Li. This study was also supported by a Taiwan Ministry Of Science and Technology (MOST) grant (103-2119-M-002-022) to C.-C. Shen.

REFERENCES

Agnihotri, R., Dutta, K., Bhushan, R., Somayajulu, B.L.K., 2002. Evidence for solar forcing on the Indian monsoon during the last millennium. *Earth and Planetary Science Letters* 198, 521–527.

Berger, A., Loutre, M.F., 1991. Insolation values for the climate of the last 10 million years. *Quaternary Sciences Review* 10, 297–317.

Berger, A.L., 1978. Long-term variations of daily insolation and Quaternary climatic changes. *Journal of the Atmospheric Sciences* 35, 2362–2367.

Blunier, T., Brook, E.J., 2001. Timing of millennial-scale climate change in Antarctica and Greenland during the last glacial period. *Science* 291, 109–112.

Bond, G., Broecker, W.S., Johnsen, S., McManus, J., Labeyrie, L., Jouzel, J., Bonani, G., 1993. Correlations between climate records from North Atlantic sediments and Greenland ice. *Letters to Nature* 365, 143–147.

Cai, Y., An, Z., Cheng, H., Edwards, R.L., Kelly, M.J., Liu, W., Wang, X., Shen, C., 2006. High-resolution absolute-dated Indian monsoon record between 53 and 36 ka from Xiaobailong cave, southwestern China. *Geology* 34, 621–624.

Castagnoli, G.C., Bonino, G., Provenzale, A., Serio, M., 1990. On the presence of regular periodicities in the thermoluminescence profile of a recent sea sediment core. *Philosophical Transactions of the Royal Society, A: Mathematical, Physical and Engineering Sciences* 330, 481–486.

Cheng, H., Edwards, R.L., Broecker, W.S., Denton, G.H., Kong, X., Wang, Y., Zhang, R., Wang, X., 2009. Ice age terminations. *Science* 326, 248–252.

Cheng, H., Edwards, R.L., Shen, C.-C., Polyak, V. J., Asmerom, Y., Woodhead, J., Hellstrom, J., Wang, Y., Kong, X., Spötl, C., 2013a. Improvements in ^{230}Th dating, ^{230}Th and ^{234}U half-life values, and U-Th isotopic measurements by multicollector inductively coupled plasma mass spectroscopy. *Earth and Planetary Science Letters* 371–372, 82–91.

Cheng, H., Sinha, A., Cruz, F.W., Wang, X., Edwards, R.L., d'Horta, F., Ribas, C.C., Vuille, M., Stott, L.D., Auler, A.S., 2013b. Climate change patterns in Amazonia and biodiversity. *Nature Communications* 4, 1411. http://dx.doi.org/10.1038/ncomms2415.

Cheng, H., Sinha, A., Wang, X., Cruz, F.W., Edwards, R.L., 2012. The global paleomonsoon as seen through speleothem records from Asia to the Americas. *Climate Dynamics* 39, 1045–1062.

Cosford, J., Qing, H., Yuan, D., Zhang, M., Holmden, C., Patterson, W., Cheng, H., 2008. Millennial-scale variability in the Asian monsoon: evidence from oxygen isotope records from stalagmites in southeastern China. *Palaeogeography, Palaeoclimatology, Palaeoecology* 266, 3–12.

Dahl-Jensen, D., Johnsen, S., 1986. Palaeotemperatures still exist in the Greenland ice sheet. *Nature* 320, 250–252.

Damon, P.E., Sonnett, C.P., 1991. Solar and terrestrial components of the atmospheric ^{14}C variation spectrum. In Sonnett, C.P., Giampapa, M.S., Matthews, M.S. (Eds.), *The Sun in Time*. University of Arizona Press, Tucson, pp. 360–388.

Dansgaard, W., 1954. The ^{18}O-abundance in fresh water. *Geochimica et Cosmochimica Acta* 6, 241–260.

Dansgaard, W., Johnsen, S.J., Clausen, H.B., Dahl-Jensen, D., Gundestrup, N.S., Hammer, C.U., Hvidberg, C.S., *et al.* 1993. Evidence for general instability of past climate from a 250-kyr ice core record. *Nature* 364, 218–220.

Ding, Y., Li, C., Liu, Y., 2004. Overview of the South China Sea Monsoon Experiment. *Advances in Atmospheric Sciences* 21, 343–360.

Duan, W., Cheng, H., Tan, M., Edwards, R.L., 2016. Onset and duration of transitions into Greenland Interstadials 15.2 and 14 in northern China constrained by an annually laminated stalagmite. *Scientific Reports* 6, 20844. http://dx.doi.org/10.1038/srep20844.

Dykoski, C.A., Edwards, R.L., Cheng, H., Yuan, D.X., Cai, Y.J., Zhang, M.L., Lin, Y.S., Qing, J.M., An, Z.S., Revenaugh, J., 2005. A high-resolution, absolute-dated Holocene and deglacial Asian monsoon record from Dongge Cave, China. *Earth and Planetary Science Letters* 233, 71–86.

https://doi.org/10.1017/qua.2017.22 Published online by Cambridge University Press

Edwards, R.L., 1988. High precision thorium-230 ages of corals and the timing of sea level fluctuation in the late Quaternary. *Earth and Planetary Science Letters* 90, 371–381.

Han, L.-Y., Li, T.-Y., Cheng, H., Edwards, R.L., Shen, C.-C., Li, H.-C., Huang, C.-X., *et al.* 2016. Potential influence of temperature changes in the Southern Hemisphere on the evolution of the Asian summer monsoon during the last glacial period. *Quaternary International* 392, 239–250.

Jaffey, A.H., Flynn, K.F., Glendenin, L.E., Bentley, W.C., Essling, A.M., 1971. Precision measurement of half-lives and specific activities of ^{235}U and ^{238}U. *Physical Review* C4, 1889–1906.

Johnsen, S.J., Clausen, H.B., Dansgaard, W., Fuhrer, K., Gundestrup, N., Hammer, C.U., Iversen, P., Jouzel, J., Stauffer, B., Steffensen, J.P., 1992. Irregular glacial interstadials recorded in a new Greenland ice core. *Nature* 359, 311–313.

Jouzel, J., Alley, R.B., Cuffey, K.M., Dansgaard, W., Grootes, P., Hoffmann, G., Johnsen, S.J., *et al.* 1997. Validity of the temperature reconstruction from water isotopes in ice cores. *Journal of Geophysical Research* 102, 26471–26487.

Laskar, J., Robutel, P., Joutel, F., Gastineau, M., Correia, A.C.M., Levrard, B., 2004. A long-term numerical solution for the insolation quantities of the Earth. *Astronomy and Astrophysics* 428, 261–285.

Leuschner, D.C., Sirocko, F., 2000. The low-latitude monsoon climate during Dansgaard/Oeschger cycles and Heinrich events. *Quaternary Science Reviews* 19, 243–254.

Li, T.-Y., Shen, C.-C., Huang, L.-J., Jiang, X.-Y., Yang, X.-L., Mii, H.-S., Lee, S.-Y., Lo, L., 2014. Stalagmite-inferred variability of the Asian summer monsoon during the penultimate glacial-interglacial period. *Climate of the Past* 10, 1211–1219.

Li, T.-Y., Shen, C.-C., Li, H.-C., Li, J.-Y., Chang, H.-W., Song, S.-R., Yuan, D.-X., *et al.* 2011. Oxygen and carbon isotopic systematics of aragonite speleothems and water in Furong Cave, Chongqing, China. *Geochimica et Cosmochimica Acta* 75, 4140–4156.

Li, T.-Y., Yuan, D.-X., Li, H.-C., Yang, Y., Wang, J.-L., Wang, X.-Y., Li, J.-Y., Qin, J.-M., Zhang, M.-L., Lin, Y.-S., 2007. High-resolution climate variability of southwest China during 57–70 ka reflected in a stalagmite δ^{18}O record from Xinya Cave. *Science in China, Series D: Earth Sciences* 50, 1202–1208.

Liu, Z., Wen, X., Brady, E.C., Otto-Bliesner, B., Yu, G., Lu, H., Cheng, H., *et al.* 2013. Chinese cave records and the East Asia Summer Monsoon. *Quaternary Science Reviews* 83, 115–128.

Lutgens, F. K., Tarbuck, E.J., 2001. *The Atmosphere* (8th ed. Prentice Hall, Englewood Cliffs, NJ.

North Greenland Ice Core Project members. 2004. High-resolution record of Northern Hemisphere climate extending into the last interglacial period. *Nature* 431, 147–151.

Paillard, D., Labeyrie, L., Yiou, P., 1996. Macintosh program performs time-series analysis. *EOS, Transactions of the American Geophysical Union* 77, 379.

Porter, S.C., An, Z., 1995. Correlation between climate events in the North Atlantic and China during the last glaciation. *Nature* 375, 305–308.

Railsback, L.B., Xiao, H., Liang, F., Akers, P.D., Brook, G.A., Dennis, W.M., Lanier, T.E., Tan, M., Cheng, H., Edwards, R.L., 2014. A stalagmite record of abrupt climate change and possible Westerlies-derived atmospheric precipitation during the Penultimate Glacial Maximum in northern China. *Palaeogeography, Palaeoclimatology, Palaeoecology* 393, 30–44.

Schulz, M., Mudelsee, M., 2002. REDFIT: estimating red-noise spectra directly from unevenly spaced paleoclimatic time series. *Computers and Geosciences* 28, 421–426.

Shen, C.-C., Wu, C.-C., Cheng, H., Edwards, R.L., Hsieh, Y.-T., Gallet, S., Chang, C.-C., *et al.* 2012. High-precision and high-resolution carbonate ^{230}Th dating by MC-ICP-MS with SEM protocols. *Geochimica et Cosmochimica Acta* 99, 71–86.

Stocker, T.F., Johnsen, S.J., 2003. A minimum thermodynamic model for the bipolar seesaw. *Paleoceanography* 18, 1087. http://dx.doi.org/10.1029/2003PA000920.

Stuiver, M., Braziunas, T.F., 1989. Atmospheric ^{14}C and century scale solar oscillations. *Nature* 338, 405–408.

Stuiver, M., Braziunas, T.F., 1993. Sun, ocean, climate and atmospheric $^{14}CO_2$: an evaluation of causal and spectral relationships. *Holocene* 3, 289–305.

Sun, Y., Clemens, S.C., Morrill, C., Lin, X., Wang, X., An, Z., 2012. Influence of Atlantic meridional overturning circulation on the East Asian winter monsoon. *Nature Geoscience* 5, 46–49.

Svensson, A., Andersen, K.K., Bigler, M., Clausen, H.B., Dahl-Jensen, D., Davies, S.M., Johnsen, S.J., *et al.* 2008. A 60 000 year Greenland stratigraphic ice core chronology. *Climate of the Past* 4, 47–57.

Taylor, S.R., McLennan, S.M., 1995. The geochemical evolution of the continental crust. *Reviews of Geophysics* 33, 241–265.

Thomas, E.R., Wolff, E.W., Mulvaney, R., Johnsen, S.J., Steffensen, J.P., Arrowsmith, C., 2009. Anatomy of a Dansgaard-Oeschger warming transition: high-resolution analysis of the North Greenland Ice Core Project ice core. *Journal of Geophysical Research: Atmospheres* 114, D08102. http://dx.doi.org/10.1029/2008 JD011215.

Voelker, A.H.L., workshop participants. 2002. Global distribution of centennial-scale records for Marine Isotope Stage (MIS) 3: a database. *Quaternary Science Reviews* 21, 1185–1212.

Wang, B., Lin, H., 2002. Rainy season of the Asian–Pacific summer monsoon. *Journal of Climate* 15, 386–396.

Wang, H.-B., Li, T.-Y., Yuan, N., Li, J.-Y., 2014. Environmental signification and the characteristics of δD and δ^{18}O variation in the local precipitation and drip water in Yangkou cave, Chongqing. [In Chinese, with English abstract.]. *Carsologica Sinica* 33, 146–155.

Wang, Y.J., Cheng, H., Edwards, R.L., An, Z.S., Wu, J.Y., Shen, C.-C., Dorale, J.A., 2001. A high-resolution absolute-dated Late Pleistocene monsoon record from Hulu Cave, China. *Science* 294, 2345–2348.

Webster, P.J., Magaña, V.O., Palmer, T.N., Shukla, J., Tomas, R.A., Yanai, M., Yasunari, T., 1998. Monsoons: processes, predictability, and the prospects for prediction. *Journal of Geophysical Research* 103, 14451–14510.

Zhang, R., Zhu, X., Han, D., Zhang, Y., Fang, F., 1998. Preliminary study on karst caves of Mt. Jinfo, Nanchuan, Chongqing. [In Chinese, with English abstract.]. *Carsologica Sinica* 17, 196–211.

Zhao, K., Wang, Y., Edwards, R.L., Cheng, H., Liu, D., 2010. High-resolution stalagmite δ^{18}O records of Asian monsoon changes in central and southern China spanning the MIS 3/2 transition. *Earth and Planetary Science Letters* 298, 191–198.

Zhao, K., Wang, Y., Edwards, R.L., Cheng, H., Liu, D., Kong, X., Ning, Y., 2016. Contribution of ENSO variability to the East Asian summer monsoon in the late Holocene. *Palaeogeography, Palaeoclimatology, Palaeoecology* 449, 510–519.

Zhou, H., Zhao, J.-X., Feng, Y., Chen, Q., Mi, X., Shen, C.-C., He, H., *et al.* 2014. Heinrich event 4 and Dansgaard/Oeschger events 5–10 recorded by high-resolution speleothem oxygen isotope data from central China. *Quaternary Research* 82, 394–404.

https://doi.org/10.1017/qua.2017.22 Published online by Cambridge University Press